studia biophysica *Volume 130 (1989) Number 1-3, p. 123 - 131*

CHARACTERIZATION OF VIRUS-RED-CELL INTERACTION BY ELECTROROTATION

J. GIMSA, C. PRITZEN, E. DONATH
Department of Biology, Humboldt University of Berlin,
Invalidenstr. 42, Berlin 1040, G.D.R.

Paper read at the XIIth Jena Symposium on TRENDS IN BIOELECTROCHEMISTRY OF BIOPOLYMERS AND MEMBRANES, September 19-24, 1988, Weimar, GDR

Virus-membrane fusion induced by a temperature increase from 4°C to 37°C caused a characteristic time dependence of the first characteristic frequency and of the rotation. An initial increase of the first characteristic frequency was followed by a decrease well below the value of the control. Rotation decreased in a characteristic manner, too. This process was terminated by hemolysis about 10 minutes after induction of fusion. The electrorotation changes were explained by a sequence of ion permeability changes.

1. Introduction

Electrorotation is a method for investigating the passive electric properties of single cells by means of a relatively simple experimental setup /1/. Cells placed in a rotating electric field with a frequency in the kHz-range spin slowly against the rotation direction of the field (anti-field-rotation). At a certain frequency, the first characteristic frequency, this anti-field-rotation is at maximum. We investigated how the anti-field-rotation peak of red blood cells was influenced by virus-cell interaction.

The first characteristic frequency as well as the peak height are strongly influenced by membrane and cytoplasm properties. In case of virus-membrane fusion a typical time dependency of the first characteristic frequency and the peak height was experimentally observed. We tried to interprete these data by introducing certain electrochemical equations relating membrane and intracellular conductivity to permeability and time dependent ion concentrations. To desribe theoretically the electrorotation behaviour the single-shell model /1/ reduced to area specific electric membrane parameters /2/ was used. While other methods like fluorescence membrane-mixing-assays or measurements of hemolysis are integrative we were able to investigate single cell events.

2. Method and Materials

Electrorotation was measured in a four-electrode chamber driven by four 90°-phase-shifted square-topped signals. The field strength within the chamber with electrode distances of 1.5 mm was about 7 kV/m. Measurements were performed after sedimentation of the cells onto a gelatine covered surface using an inverted microscope. The first characteristic frequency of the cell under investigation was followed by a compensation method /3/. At different times rotation speed at the characteristic frequency was determined by switching the compensation field to a simple rotation field. For measurements human red blood cells stored no longer than three days in ACD medium and Influenza-viruses (strain A/PR 8/34) were used. To ensure virus adsorption cells were incubated in Influenza-virus suspension of 2µg virus protein/ml for about 5 minutes at 0°C. After this the cells were transferred to the measuring chamber. Cell concentrations of about 0.02% were used. The first characteristic frequency of one and the same cell was followed for several minutes. pH was calibrated to 5.2 or 5.8 with phosphate-buffer. Isotonicity was ensured by addition of 300 mOsm saccharose. Measurements were carried out on about 20 cells in each solution at a temperature of about 37°C. External conductivities of about 0.01 S/m corresponding to approximately 1 mM salt were used.

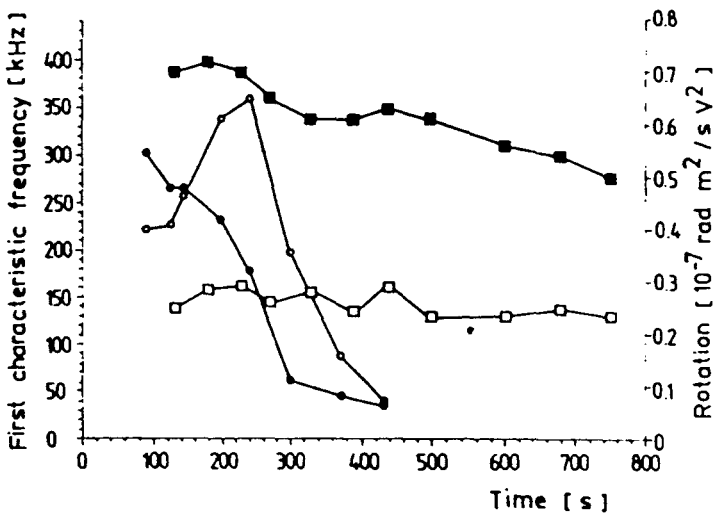

FIG.1
Time dependency of the first characteristic frequency (open symbols) and the rotation (filled symbols) of two typical cells

circles:
pH 5.2, external conductivity 0.0112 S/m

squares:
pH 5.8, external conductivity 0.0083 S/m

3. Experimental results

Fig. 1 shows that the time dependency of the first characteristic frequency and the rotation strongly depended on pH. Parallel fluorescence membrane-mixing-assays showed that the strong decrease of rotation and the initial increase of the first characteristic frequency followed by a strong decrease was observed only when fusion of virus envelope and cell membrane was present /4, 5/. This was the case only at pH 5.2 but not at pH 5.8. We observed that if the fluorescence membrane-mixing-assay detected a 50%-value for virus-cell fusion half of the population had fused to 100%.

4. Discussion

In the following we will consider the time dependence of the anti-field-rotation peak for the case of fusion using simple electrochemical equations to express the conductivities of cytoplasm and membrane by permeabilities and concentrations. These expressions were inserted into the single-shell model. For our considerations we assumed red blood cells as homogeneous spheres covered by the membrane. The torque of the anti-field rotation N, of such a single-shell sphere is described by:

$$N=4\pi\epsilon_m\epsilon_0 r^3 E^2 \left(\frac{C_1}{C_2}-\frac{B_1}{B_2}\right)\frac{f/f_{c1}}{1+(f/f_{c1})^2} \qquad \text{with } f_{c1}=C_2/2\pi B_2 \qquad (1)$$

Where ϵ_m, ϵ_0 - dielectric constant of the external solution and absolute permittivity of vacuum, r - cell radius, E - external field strength, f - field frequency, f_{c1} - first characteristic frequency and B_1, B_2, C_1, C_2 are constants.

Using area specific values for the membrane electric properties /2/ the C- and B-constants read:

$$\begin{aligned} B_1&=C_m(G_i-G_m)\\ B_2&=C_m(G_i+2G_m)\\ C_1&=G_m(G_i-G_m)-G_iG_m/r\\ C_2&=G_m(G_i+2G_m)+2G_iG_m/r \end{aligned} \qquad (2)$$

Where G_m is the membrane conductivity per unit area and G_i, G_m are the internal and external specific conductivities, respectively. C_m is the membrane capacity per unit area.
After checking the possible influence of osmotically induced volume changes on the rotation behaviour we came to the conclusion that the observed increase of the first characteristic frequency caused by virus-membrane interaction can only be the

result of an increase of membrane conductivity. Using equations (1) and (2) the first characteristic frequency can be written as:

$$f_{c1} = \frac{G_m}{2\pi C_m} + \frac{1}{2\pi r C_m (1/2G_m + 1/G_i)} \quad (3)$$

The cell volume can only vary in a range of 0.6 up to 1.6 of the physiological cell volume. The lower limit is determined by an osmotically inactive volume, the upper one by hemolysis. Radius changes resulting from such volume changes are to small to quantitatively explain the observed changes of the first characteristic frequency. Although there is a small influence of radius changes on measured data we assumed for further calculations the cell radius to be constant equal to 3 μm. The membrane capacity was determined from control experiments to be 0.56 $\mu F/cm^2$ /1, 2/. According to /6/ the area specific membrane conductivity G_m measured in S/m^2 can be expressed in terms of permeabilities and ion concentrations c^m:

$$G_m = \sum_i \frac{P_i (z_i F)^2}{RT} c_i^T \quad (4)$$

Where R and T are the gas constant and temperature; F is FARADAYs constant, c_i^T is the average concentration of the ionic species i with charge number z_i and permeability P_i.

The average ion concentration entering eq. 4 was assumed to be half the value of the sum of external and internal concentration of the considered ion. This assumption does not mean that the membrane concentration is proportional to the average bulk concentration. It rather takes into account that the membrane conductivity may depend on the direction of the applied electric field and yields an average G_m in eq. 4. Because of the very low cell concentration the external concentration is constant and equals 1 mM NaCl. In our calculations we considered only permeabilities and concentrations of monovalent cations, Na^+ and K^+ and anions, Cl^-. Additionally we took into account the exchange permeability of Cl^--ions, $2*10^{-6}$ m/s. The internal conductivity G_i is connected with the intracellular concentration, c^i:

$$G_i = Lc^i/2 \quad (5)$$

Where L is the equivalent conductivity of the pure electrolyte. We neglected the concentration dependence of L. L was equal to 0.01 S/m^2/equiv.. Since Pauly and Schwan /7/ found that the cytoplasmic ionic mobility was reduced by ion-hemoglobin interaction to about 50% as compared with pure electrolyte we introduced in (5) a factor of two. The time dependence of the internal ion concentration c^i was described by:

$$c^i = c^e + (c^{i\circ} - c^e)\exp(-3tP_{ion}/r) \quad (6)$$

c^e, $c^{i\circ}$, t and P_{ion} stand for external salt concentration, internal salt concentration at time t=0 (154 mM), time and the permeability limiting the net efflux of salt. Because electrorotation cannot distinguish between positively and negatively charged ions for simplification we assumed that anions have the smallest net permeability, $P_{ion}=P_{anion}$.
To simulate the anti-field rotation dependence as a function of time we plotted the first characteristic frequency and the normalized torque against time (see Fig. 2 and 3).
If we consider the induction of a permeability increase by virus fusion there are two main effects: First, an increase of the membrane permeability will lead to ion leakage and a subsequent decrease of the intracellular ion concentration. Second, intracellular ion concentration changes influence ion partition or ion binding to membrane sites. This may cause in turn changes of the membrane conductivity G_m.
One can estimate immediately that the range of virus induced leakage permeabilities should be of the order of 10^{-7} to 10^{-6} m/s: First, the time for the decrease of the first characteristic frequency shown in Fig. 1 reflecting the loss of ions from cytoplasm and the decrease of the internal conductivity can only be explained by a permeability within this range. Second, from the time of hemolysis we concluded that the final saccharose permeability is of the order of 10^{-9} m/s. Therefor it is reasonable to assume ionic permeabilities to be one to three orders of magnitude higher.

The simplest possible case we simulated was the induction of a permeability increase to a constant value due to virus fusion. The assumption of a step permeability increase equal for all ion species induced by virus-membrane fusion at the time of temperature increase (t=0) leads to an exponential decrease of internal conductivity and membrane concentration of ions. This can only cause a decrease of f_{c1} and of the torque (see Fig. 2, curves 1-2).
Since this simplest case did even not qualitatively explain the experimentally observed behaviour we further studied electrorotation changes predicted when the permeability exponentially increased with time following virus-membrane fusion. As shown in curve 3 in Fig. 2 even this more sophisticated assumption cannot explain the measured time dependence of the first characteristic frequency either. Because of the assumed equal permeabilities for cations and anions increasing permeabilities caused a loss of ions from the interior which resulted only in a drop of the first

characteristic frequency. The increase of the membrane conductivity calculated according to equation (3) cannot compete for the decrease of intracellular conductivity. The torque qualitatively behaved like in the case of the step induction of a permeability to a constant value.

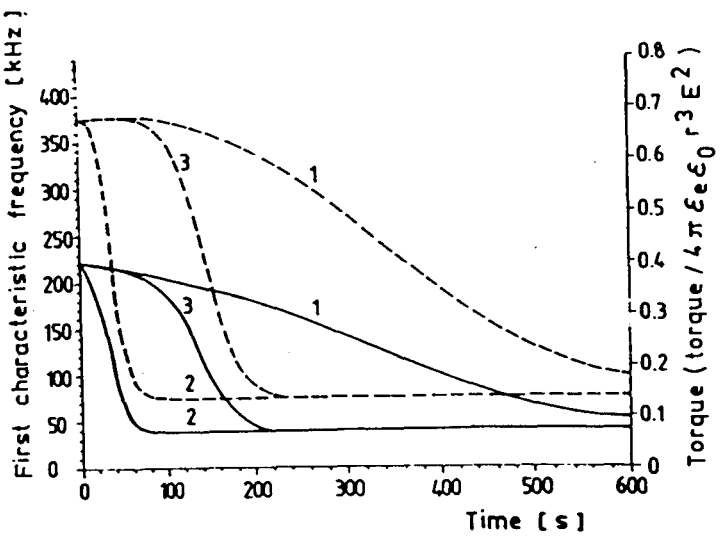

FIG. 2
Time dependency of first characteristic frequency (-----) and torque (- - -)
A step-like increase of the membrane permeabilities for anions and cations at t=0 were assumed for curve 1 ($P=10^{-8}$ m/s) and 2 ($P=10^{-7}$ m/s). An exponentially increasing permeability for anions and cations (from 10^{-11} to 10^{-7} m/s), with a characteristic time of 500 s was assumed for curve 3

Hence, to explain the experimentally observed increase of the first characteristic frequency, the membrane conductivity must increase while the internal conductivity should not decrease as fast as in Fig. 2. This was only possible if different permeabilities for cations and anions were introduced (see Fig. 3). In this case the increasing permeability of one ion species would increase the membrane conductivity but leakage of ions cannot take place because a membrane potential difference is generated.

In order to get deeper insight into the reasons for the time-dependence of the anti-field rotation in case of membrane permeability changes we calculated a network diagram for the torque and the first characteristic frequency (see Fig. 4). As parameters we used the intracellular conductivity and the membrane conductivity, respectively. Considering the influence of the internal conductivity on the torque and on the first characteristic frequency from Fig. 4 it is obvious that for an internal coductivity change in case that the internal conductivity is much

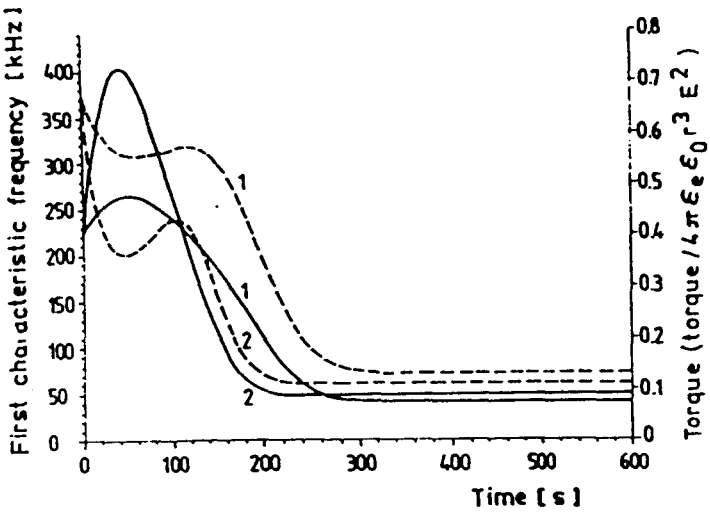

FIG. 3
Time dependency of first characteristic frequency (-----) and torque (- - -) for sequentially increasing permeabilities measured in m/s

	cations			anions		
curve	charact. time (s)	starting at	ending at	charact. time (s)	starting at	ending at
1-	100	10^{-11}	$2*10^{-5}$	1000	10^{-9}	10^{-7}
2-	100	10^{-11}	10^{-4}	500	10^{-9}	10^{-7}

higher than the external conductivity both parameters change only slightly. A drop to half of the conductivity value within this range changes the torque and the first characteristic frequency much less than the same drop for the case that the internal conductivity is already within the range of the external conductivity. Considering the membrane conductivity one observes that it changes the electrorotation parameters, torque and first characteristic frequency, throughout its possible range except very low conductivities in an equal manner. How can now the cell behaviour be explained with the help of Fig. 4? A membrane permeability increase can only cause a decrease of the internal conductivity. This process should be accompanied by a decrease of torque and the first characteristic frequency. But a permeability increase is also connected to a membrane conductivity increase, as long as enough ions within the cell are present to carry a current through the membrane. This causes in the case of a sequential permeability increase in turn an increase of the first characteristic frequency large enough to compete the small effect of

the decrease of the intracellular conductivity. The trajectory of a cell is shifted from somewhere in the upper corner rightward down almost parallel to the internal conductivity coordinate planes. Since the internal conductivity decreases continuously limited by the anion (or cation) permeability there must be later on a membrane conductivity decrease. too (see eq. 4). The trajectory of the cell now starts to go back leftward. Since the coordinate planes in diagram 4 are bended leftward up a decrease of the membrane conductivity will cause a transient increase in torque. This interpretation qualitatively explains the theoretical curves in Fig. 3.

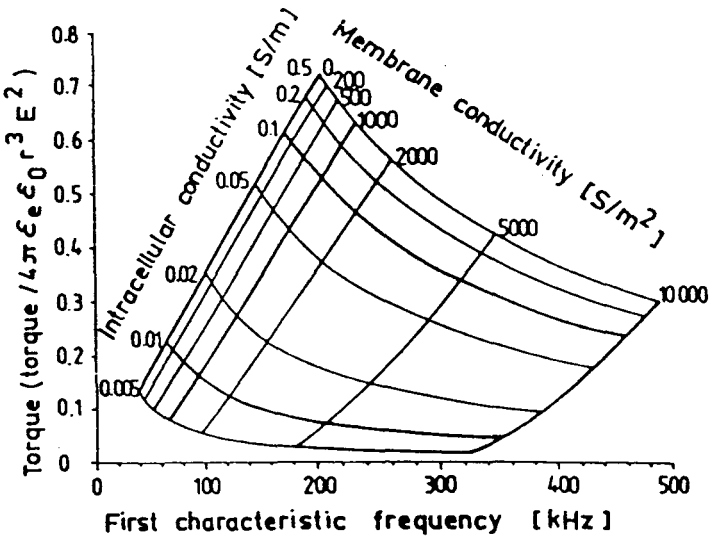

FIG. 4
Network diagram of torque and first characteristic frequency.
For calculations according to equation (1) a cell radius of 3 μm, a membrane capacity of 0.56 μF/cm^2 and an external conductivity of 0.0112 S/m was assumed

3. Conclusions

Hence, to explain the experimentally observed increase of the first characteristic frequency together with the behaviour of the torque was only possible if different permeabilities for cations and anions were introduced. A sequential permeability increase induced by Influenza-viruses was already described by Pasternak et al. /8/. The observed lag phase in the first characteristic frequency increase not discussed yet may be due to delayed fusion or to a more sophisticated dependence of permeability on time as discussed here. We are aware that our consideration can only be a

first approach but it nevertheless shows that investigations of electrorotation of single cells offer new possibilities to study biological processes by means of interpreting membrane dielectric data with the help of electrochemical approaches.

Acknowledgement

We thank Dr. A. Herrmann and Prof. Dr. Glaser for helpful discussions and their interest for the advance of this paper.

References

/1/ GLASER, R., FUHR, G., 1987. in: BLANK, M., FINDL, E., Mechanistic Approaches to Interactions of Electric and Electromagnetic Fields with Living Systems. Plenum Press. N.Y.
/2/ GIMSA, J., DONATH, E., GLASER, R. Bioelectrochem. Bioenerg. 19 (1988) 389
/3/ ARNOLD, W.M., ZIMMERMANN, U., Patent DE 3325843 A1
/4/ STEGMANN, T., HOEKSTRA, D., SCHERPHOF, G. WILSCHUT, J., J. Biol. Chem. 261 (1986) 10966
/5/ PRITZEN, C., HERRMANN, A., Bioscience Rep. 8 (1988) 55
/6/ ENGEL, J., DONATH, E., GIMSA, J., stud. biophys. 125 (1988) 53
/7/ PAULY, H., SCHWAN, H. P., Biophys. J. 6 (1966) 622
/8/ PASTERNAK, C.A., ALDER, G.M., BASHFORD, C.L., BUCKLEY, C.D. MICKLEM, C.J., PATEL, K., Biochim. Soc. Symp. 50 (1985) 247

Dr. J. GIMSA, Department of Biology, Humboldt University of Berlin, Invalidenstr. 42, DDR-1040 Berlin, GDR